Available online at www.sciencedirect.com
SCIENCE DIRECT®
Journal of Power Sources 127 (2004) 181–186
JOURNAL OF POWER SOURCES
www.elsevier.com/locate/jpowsour

Cell voltage transients of a gas-fed direct methanol fuel cell

Josef Kallo [a,*], Jim Kamara [a], Werner Lehnert [b], Rittmar von Helmolt [a]

[a] *GM-FCA, Peter Sander Str. 43, 55252 Mainz Kastel, Germany*
[b] *ZSW ULM, Helmholtz Str. 8, 89081, Ulm, Germany*

Abstract

The cell voltage behavior of a direct methanol fuel cell (DMFC) was investigated in response to the dynamic change of the cell current (current steps with rise/decay time = 1 ms). The cell voltage was measured on a complete cell under regular fuel cell working conditions. To minimize the methanol cross-over from the anode to the cathode and its influence on the dynamic cell behavior, the anode feed of the DMFC was kept gaseous. The cell voltage transient permits a differentiation of three influencing effects on the cell dynamic: (1) the double layer capacity and the charge transfer resistance of the anode and the cathode, (2) the CH_3OH dehydrogenation products poisoning of and its removal from the anode catalyst surface and (3) the impact of the remaining methanol cross-over. Contrary to the first two effects, which take place in the time range of 50 ms to 1 s, the methanol cross-over influences the cell voltage for approximately 10 s after the current changes.

Keywords: Dynamic fuel cell; Transient; Gaseous direct methanol fuel cell; DMFC

1. Introduction

Publications describing the cell voltage behavior of a direct methanol fuel cell (DMFC) under dynamic load conditions are sparse. Argyropoulos [1,2] enumerates the influencing parameters for a liquid-fed DMFC and shows experimentally the impact of anode concentration, flow and cathode pressure on the dynamic cell response. Together with Simoglou and Argyropoulos [3,4] they presented a canonical variate analysis (CVA) state space model to predict the generic behavior of the liquid DMFC based on special dynamic experimental data. Kulikovski [5] describes analytically the gas dynamics in channels of a gas-fed DMFC and Sundmacher and Schultz [6] show a mathematical approach for the liquid DMFC under dynamic load conditions. Finally, the work of Lee and Eickes [7], which describes the electrochemical oscillations in the methanol oxidation on Pt, should be mentioned.

In our work we present experimental data for cell voltage response under dynamic load conditions for a gas-fed DMFC. Further we differentiate the cell voltage response in three specific effects including the double layer impact, the formation/removal of CO at the anode and the influence of the methanol cross-over from the anode to the cathode for different methanol concentrations at the anode.

The gas-fed DMFC we used minimizes the impact of mass transfer to the anode catalyst due to the much higher diffusion coefficient of the species in a gas phase compared to a liquid one. The CO_2 removal therefore also has an insignificant impact on the dynamic cell behavior. We know from our former work [8] that the methanol diffusion from the anode to the cathode for a gas-fed DMFC is only 50% of that for a liquid one. That means the impact of methanol oxidation at the cathode on the dynamic behavior of the cell is smaller for a gas-fed DMFC. Further we also can neglect in a first approach the influence of the reaction heat release and its impact on phase conversion (liquid → gaseous), because of the presence of a single phase at the anode catalyst. As shown in [8], the cathode pressure and temperature has to ensure a good membrane conductivity. For the experiments described here, conditions were chosen with partially humidified air at the inlet (relative humidity at the inlet RHin ≈ 57%).

2. Experimental

The fuel cell used in this work was a single cell (active area 100 mm × 100 mm). The supplied membrane electrode assemblies (MEAs) were prefabricated from Nafion117 with Toray paper for diffusion media. The catalysts used were Pt/Ru on the anode side and Pt on the cathode side. The graphite cell used (10 mm thick, 130 mm × 130 mm) had a

* Corresponding author.
E-mail address: josef.kallo@de.opel.com (J. Kallo).

0378-7753/$ – see front matter © 2003 Elsevier B.V. All rights reserved.
doi:10.1016/j.jpowsour.2003.09.014

Nomenclature

c_{i1}	particle concentration at low current density
c_{i2}	particle concentration for very high current density
$D_{ik,eff}$	effective diffusion coefficient of species "*i*"
$j_{DA/C}$	charge transfer current for anode/cathode
J_i	particle current density
$K_{A/C}$	constant depending on temperature, electrochemical reaction symmetry, and electron reaction-number
l_0	membrane thickness (180 μm)
MEA	membrane electrode assembly
RHin	relative humidity at the inlet
R_{DA}	charge transfer resistance of the anode
R_{DC}	charge transfer resistance of the cathode
$x = 0$	anode side
$x = l_0$	cathode side

serpentine flow field with five parallel channels (width = 1 mm, depth = 1 mm). The gas supply direction was of co-flow type (i.e. same flow direction in the anode and cathode channels). The electric connection was performed with 1 mm thick copper plates pressed between the graphite flow field and the isolated aluminum end plates. The cell sealing was made on each side of the MEA with a Teflon frame adjusted to the diffusion media thickness. The temperature control of the cell was achieved by heating up the aluminum end plates. The temperature measurement took place in the middle of the flow field plate, 3 mm under the flow field channels. The temperature of the end plates was also limited to a degree above cell temperature, to avoid overheating of the cell during the start-up procedure. At the inlet of the anode, the methanol/water mixture had to be gaseous. Therefore, the liquid anode mixture was pressurized at room temperature with nitrogen and, after controlling the mass flow with an liquiflow controller (Bronkhorst), injected into a vaporizer. The dissolved nitrogen gas (0.015 g/dm^3 at room temperature) was neglected as part of the anode flow. The vaporizer outlet temperature exceeded 140 °C. The connection tube between the vaporizer outlet and the cell inlet was also heated to 20 K above the cell temperature. Consequently it could be ensured that no condensation took place before the cell. The gas humidification on the cathode side was performed by conducting the air through a heated stainless steel cylinder filled with water. The connection tube between humidifier and cathode cell inlet was also heated to 5–8 K above the dew point temperature of the cathode. The pressure set points of the cathode and anode could be adjusted independently from each other. For comparison the cell could be operated with humidified hydrogen at the anode.

The cell load was taken on a Höcherl & Hackl DS406 SV3 electronic load, programmed with National Instruments LabView. A minimum rise and decay time of 100 μs were ensured. The minimum rise/decay time we used was 1 ms. To control the current signal we used a LEM (HAL150-S/SP2) current-to-voltage converter and measured this voltage and the cell voltage with a DSPACE A/D converter using a 10 kHz sampling rate.

3. Results and discussion

As mentioned in the introduction, we look closer at the cell voltage response of a gas-fed DMFC for dynamic (rise/decay time $\Delta t = 1$ ms) current density change. To differentiate the gas-fed DMFC from other gas-fed fuel cells (anode fuel = hydrogen), the voltage response for a gas-fed DMFC is compared in Fig. 1 with the voltage response of the same cell, fueled only with humidified hydrogen. As seen in Fig. 1, the open circuit voltage and the cell voltage under load is smaller for the DMFC compared with the hydrogen fueled cell, due to methanol cross-over and mixed potential at the cathode. It is apparent that the DMFC has a different characteristic of the cell voltage after a current density change. For increasing current density the cell voltage of the DMFC shows a temporarily smaller value before recovering to a constant value. For decreasing current densities the voltage rises to a temporarily higher value than the open circuit voltage. This behavior is already described for a liquid phase DMFC in [1,2] and identified as the influence of different mixed potentials at the cathode, due to varying methanol cross-over flow densities. But compared with [1], it takes approximately 10 s instead of 100 s to reach a stable cell voltage value. We assume this is the result of the fast species distribution through the diffusion media in the gas phase. For this time range, only the effect of methanol diffusion through the membrane affects the cell voltage performance. We will explore this in more detail below.

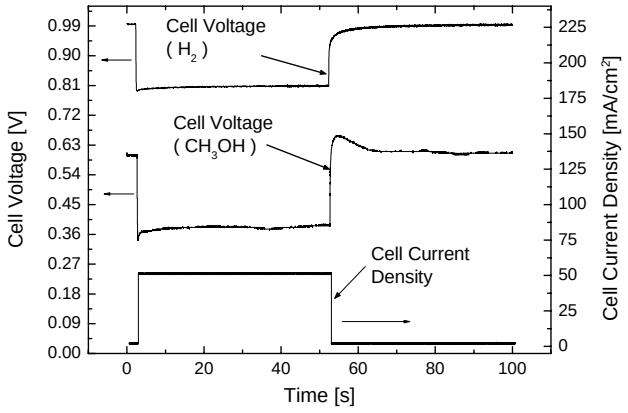

Fig. 1. Voltage response and current density for the gas-fed DMFC and for the hydrogen fueled cell. (Anode flow: 100 g/h CH_3OH/H_2O 8.25 wt.% (2.5 m) or 20 Nl/h (normal liters per hour) H_2 + 100 g/h H_2O, cathode flow: 120 Nl/h air, anode pressure: 1.96 bar, cathode pressure: 2 bar, RHin cathode: 57%, ϕ cell temperature = 119.25 °C.)

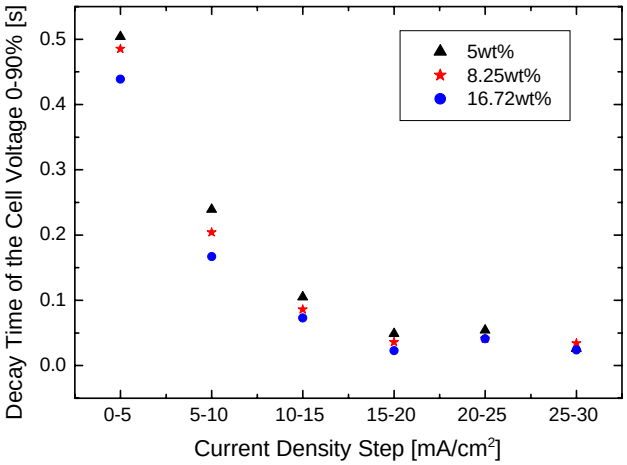

Fig. 2. Decay time of the cell voltage for constant value of the current density step and increasing start value of the current density with the anode concentration as parameter. (Anode flow: 100 g/h CH_3OH/H_2O 5 wt.% (1.5 m) or 8.25 wt.% (2.5 m) or 16.72 wt.% (5 m), cathode flow: 120 Nl/h air, anode pressure: 2 bar, cathode pressure: 2 bar, RHin cathode: 57%.)

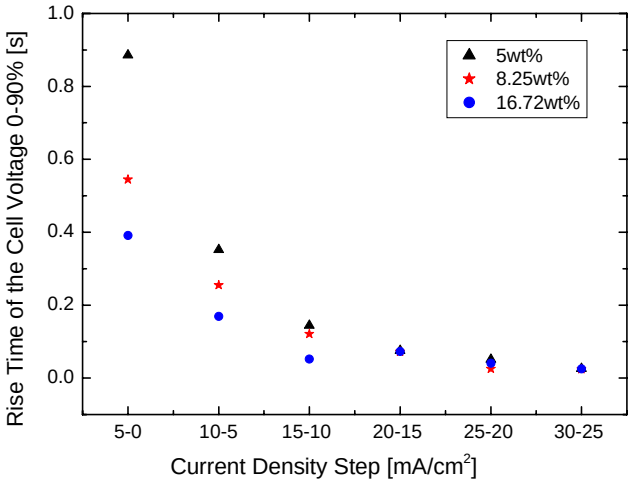

Fig. 3. Rise time of the cell voltage for constant value of the current density step and decreasing start value of the current density with the anode concentration as parameter. (Anode flow: 100 g/h CH_3OH/H_2O 5 wt.% (1.5 m) or 8.25 wt.% (2.5 m) or 16.72 wt.% (5 m), cathode flow: 120 Nl/h air, anode pressure: 2 bar, cathode pressure: 2 bar, RHin cathode: 57%.)

The cell voltage behavior of the hydrogen fueled cell shows capacitor characteristics for decreasing current densities. Consequently we look first at the rise and decay times of the cell voltage for the gas-fed DMFC.

3.1. Capacitor characteristics

According to [12] the equivalent circuit for a gas-fed DMFC can be simplified to a series connection of the membrane resistance and two capacitor/resistance parallel circuits corresponding to the double layer capacitance and the charge transfer resistance for the anode and cathode, respectively. From Hamann and Vielstich [13] we know that the charge transfer resistance of the anode R_{DA} and cathode R_{DC} is a function of the cell current with $R_{DA} = K_A(1/j_{DA})$ and $R_{DC} = K_C(1/j_{DC})$ ($K_{A/C}$: constant depending on temperature, electrochemical reaction symmetry, electron reaction-number, $j_{DA/C}$: charge transfer current for anode/cathode). In contrast to the hydrogen-fueled cell the charge transfer resistance of the anode is on the order of that of the cathode so the dynamic cell voltage measured summarizes the anode and cathode behavior. Fig. 2 shows the 0–90% *decay time* of the cell voltage after IR correction for different current density steps and different methanol concentrations at the anode. First we look at the curve for 5 wt.%. With increasing current density the decay time decreases rapidly. This can be explained with the decrease of the charge transfer resistance on both anode and cathode sides, leading to a higher self discharge current density of the double layer capacitance and to a shorter decay time of the cell voltage. Further, Fig. 2 shows the impact of the anode methanol concentration on the decay time. With increasing concentration, the methanol cross-over from the anode to the cathode increases as well. The result is a lower cell voltage and a higher parasitic current density [14], based on the methanol oxidation at the cathode. Therefore, a higher parasitic oxygen reduction current is also needed to equalize it. That means the useful cell current density starts at a lower charge transfer resistance, which for its part leads to a faster discharge of the double layer capacitance. Fig. 3 shows the 0–90% *rise* time (relaxation time) of the cell voltage after a current density reduction. (The data was first IR corrected.) It can be seen that the relaxation time for decreasing current density takes longer than for an increasing load. This effect is based on the nonlinear behavior of the charge transfer resistance which makes the relaxation time for the double layer capacitance dependent on the end value of the current density. The pronounced difference in relaxation time for the varying anode concentrations at low current densities is remarkable. Hence we conclude that the anode reaction during the voltage relaxation is different from that of the current density increase. We know from Jusys and Kaiser [9] that adsorbed CO is the stable end product of CH_3OH dehydrogenation on Pt-Ru anode catalysts. We assume that for increasing current densities, the required Pt-Ru area for methanol dehydrogenation increases also. If the former unused area is poisoned with adsorbed CO and CO precursors [9], first these have to be oxidized through an energy-intensive step including water dissociation [11]. This reaction affects the charge transfer resistance and is mostly independent of the anode methanol concentration. The adsorbed concentrations on the catalyst surface are decisive. For decreasing current densities, there is more free catalyst area than needed for the complete methanol oxidation, so the methanol adsorption and the first dehydrogenation step are the main reactions. This step defines the charge transfer resistance and is dependent on the

anode methanol concentration. This removal/poisoning effect for dynamic current density changes can be also deduced from the analysis of the cell voltage amplitude. The number of free catalyst places is smaller for a poisoned surface, leading to a higher reaction overvoltage than for a clean surface.

3.2. Catalyst cleaning/poisoning effect

As mentioned above, we assume that the adsorbed dehydrogenation products on the anode catalyst play a major role on cell voltage behavior as current density changes. Ishikawa summarizes in his work [11] the adsorption energies, the dissociation energies and the activation barriers for each CH_3OH dehydrogenation step, for the water dissociation and for the CO_{ads} oxidation. Thus the adsorption energy of CH_3OH on $(Pt_3)(Ru_4Pt_3)$ is around 0.32 eV, that of CO 1.6 eV, that of CH_2OH 2.37 eV, that of CHOH 3.33 eV, that of CHO 2.64 eV and that of water around 0.19 eV. The activation energies are 0.29 eV for the formation of CH_2OH_{ads}, 0.66 eV for the formation of $CHOH_{ads}$ and 0.84 eV for the formation of OH_{ads} from H_2O_{ads}. We know from Müller [16] that the desorption of CO_{ads} starts at temperature below 120 °C, so we can conclude that in addition to the mainly adsorbed CO_{ads}, the catalyst surface should also be covered with CH_2OH_{ads}, due to the higher adsorption energy compared to CO_{ads}, the low activation energy for its formation from CH_3OH and the high activation energy for its decomposition to $CHOH_{ads} + H_{ads}$. Because of the small adsorption energy of water, the H_2O molecules are displaced by the species mentioned before.

Fig. 4 shows the cell voltage behavior for increasing and decreasing current density. For increasing and decreasing load a "fast" ($\Delta t < 1$ s) and a "slow" ($\Delta t < 10$ s) characteristics of the cell voltage can be seen. We analyze the "fast" effect first.

Starting from a catalyst surface poisoned with CO_{ads} and CH_2OH_{ads}, the additional cell current is first produced from the adsorbed poisoning species. This species needs a high over-voltage to be oxidized. After cleaning the catalyst there is additional free area for the water dissociation, for the methanol adsorption and entire dehydrogenation. Therefore, the cell voltage drops first to a low value (2) during the catalyst cleaning and afterwards increases to an intermediate state (3).

For decreasing load, the catalyst surface is more than enough to deliver the lower current density. We assume that the excess catalyst is first poisoned with CH_2OH_{ads}, later with CO_{ads}, delivering a fraction of the current density. This current density fraction is produced with less over-voltage because the energy-intensive steps of CH_2OH_{ads} decomposition and the OH supply are not needed for each adsorbed CH_3OH molecule. Therefore, the cell voltage increases during the catalyst poisoning (5) and drops to an intermediate state (6), when the lower current density has to be generated from the complete methanol dehydrogenation and the CO_{ads} oxidation.

3.3. Methanol cross-over effect

As already mentioned, we assume that the methanol cross-over effect can affect the cell voltage behavior for dynamic current density changes. We know from our further work [8,15] that the methanol cross-over decreases for constant anode flow and concentration with increasing cell current density, so we expect a change of the mixed potential at the cathode [14]. A value of 1.56×10^{-9} m^2/s for the methanol diffusion coefficient through Nafion117 is found by Barragán [17] for temperatures around 120 °C and pressures < 2 bar. A simple estimation [10] of the time-dependent particle current density, based on Fick's first and second diffusion equations,

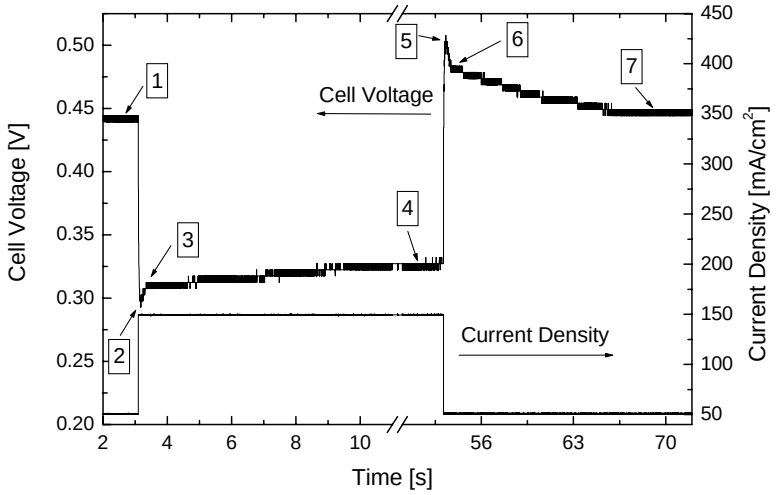

Fig. 4. Dynamic behavior of the cell voltage for a current density step. (Anode flow: 100 g/h CH_3OH/H_2O or 8.25 wt.% (2.5 m), cathode flow: 120 Nl/h air, anode pressure: 2 bar, cathode pressure: 2 bar, RHin cathode: 57%, ϕ cell temperature = 119.25 °C.)

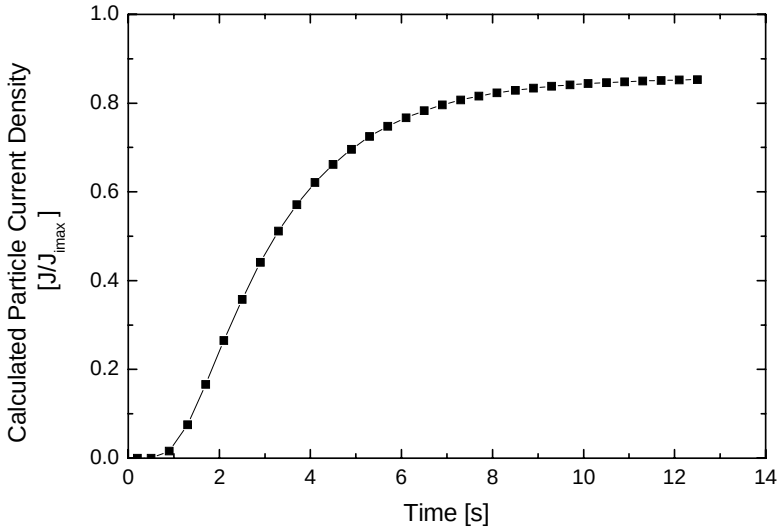

Fig. 5. Calculated particle current density (methanol) trough the Nafion117 membrane for dynamic current density decrease. ($D_{ik,eff} = 1.56 \times 10^{-9}$ m^2/s, $l_0 = 180\,\mu$m, $c_{i2} = 0$, $c_{i1} = f(j_{DA})$.)

leads to:

$$J_i(x = l_0, t) = D_{ik,eff} \frac{c_i(x = 0, t) - c_i(x = l_0, t)}{l_0} \times \left(1 + 2\sum_{m=1}^{\infty} \cos(m\pi) e^{-tm^2\pi^2 D_{ik,eff} l_0^2}\right)$$

with the following boundary and start conditions:

$$c_i(x = 0, t) = c_{i1}, \quad t > 0$$
$$c_i(x, t = 0) = c_{i2}, \quad 0 \le x \le l_0$$
$$c_i(x = l_0, t) = c_{i2}, \quad t \ge 0$$

where J_i: particle current density, c_{i1}: particle concentration at low current density, c_{i2}: particle concentration for very high current density, $x = 0$ anode side, $x = l_0$ cathode side, l_0 membrane thickness (180 μm), $D_{ik,eff}$ effective diffusion coefficient of species "i".

Fig. 5 shows the time-dependent behavior of the particle current density, calculated at $x = l_0$ with $D_{ik,eff} = 1.56 \times 10^{-9}$ m^2/s. It can be seen that the time characteristics of the particle current density are in the same time range as the cell voltage increase effect (3) → (4) and decrease (6) → (7), respectively, after a current density change. So we conclude that the methanol cross-over effect influences the cell voltage behavior in the range of $t < 10$ s after a current density change.

4. Summary

Compared with the liquid-fed direct methanol fuel cell, the vapor-fed DMFC has a couple of advantages concerning the evaluation and interpretation of the cell voltage behavior after dynamic ($\Delta t = 1$ ms) current density changes. According to its fast transport properties, we assume that the methanol–water supply and the CO_2 release do not play a major role on the cell voltage evolution under a dynamic load change. Furthermore the reaction heat plays a minor role because of the lack of two phases at the anode, thus the phase transition effects are non-existent. Finally, the smaller methanol cross-over can be enumerated, implicating a minor peculiarity of the cathode mixed potential. Under these boundary conditions, we could identify three major effects which influence the cell voltage behavior during current density change. First is the double layer capacity of the anode and cathode. Compared to the hydrogen fueled cell, the anode charge transfer resistance for the DMFC does not bypass the anode double layer, so the capacitor can buffer the cell current for 50–1000 ms, depending on current density amplitude and anode methanol concentration. That means the anode reactant delivery time can be slower.

The second effect to specify is the poisoning/cleaning of the anode catalyst. Due to the different reactions which are taking place, the charge transfer resistances are different for increasing and decreasing current densities, leading to other cell voltage characteristics. For decreasing load, the cell voltage is temporarily better than for the intermediate state, but for increasing current density the voltage falls under that of the respective intermediate state. We used a Pt/Ru alloy catalyst on the anode side. For future investigations it would be interesting to see if the specific addition of a third metal which improves the dehydrogenation of CH_2OH_{ads}, or a micro-structured catalyst which improves the supply of OH_{ads}, will suppress the evolution of that low cell voltage behavior for increasing current densities.

The third effect which influences the cell voltage behavior after current density changes is the impact of cross-over methanol. In contrast to the double layer effect its impact is observable for about 10 s. For liquid-fed DMFCs the influence may be longer, based on the slower diffusion through

the catalyst layer and the higher methanol density and storage capacity of the volume preliminary to the membrane.

References

[1] P. Argyropoulos, K. Scott, J. Power Sources 87 (2000) 153.
[2] P. Argyropoulos, K. Scott, Electrochimica Acta 45 (2000) 1983.
[3] A. Simoglou, P. Argyropoulos, Chem. Eng. Sci. 56 (2001) 6761.
[4] A. Simoglou, P. Argyropoulos, Chem. Eng. Sci. 56 (2001) 6773.
[5] A.A. Kulikovsky, Electrochem. Commun. 3 (2001) 572.
[6] K. Sundmacher, T. Schultz, Chem. Eng. Sci. 56 (2001) 333.
[7] J. Lee, C. Eickes, Electrochimica Acta 47 (2002) 2297.
[8] J. Kallo, W. Lehnert, R.V. Helmolt, J. Electrochem. Soc., in press.
[9] Z. Jusys, J. Kaiser, Electrochimica Acta 00 (2002) 1.
[10] G. Merziger, T. Wirth, Repetitorium der Höheren Mathematik, 2. Auflage, Binomi Verlag, Springe, 1993, p. 418ff.
[11] Y. Ishikawa, M.-S. Liao, C.R. Cabrera, Surface Sci. 463 (2000) 66.
[12] S. Gottesfeld, T.A. Zawodzinski, Advances in Electrochemical Science and Engineering, vol. 5, Wiley-VCH, Weinheim, 1997, p. 218.
[13] C.H. Hamann, W. Vielstich, Electrochemie, vol. 3, Wiley-VCH, Weinheim, 1998, p. 154ff.
[14] M. Messerschmidt, Mathematische Modelierung der Reaktionschichten der flüssigen Direktmethanolbrennstoffzelle, Diplomarbeit, DLR-Stuttgart, 2000.
[15] J. Kallo, J. Kamara, Performance and Dynamic Load Response of a Gas-Fed DMFC, Poster 8th UECT, Ulm 2002.
[16] B. Müller, Kohlenmonoxid-Vergiftung von Katalysatoren in der Polymerelektrolyt Brennstoffzelle, Fortschr.-Ber. VDI R.6 Nr.466, VDI Verlag, Düsseldorf (2001).
[17] V.M. Barragán, A. Heinzel, J. Power Sources 104 (2002) 66.